Analysis of the segmental stability of helical peptides by isotope-edited infrared spectroscopy

ARTICLE *in* PROTEINS STRUCTURE FUNCTION AND BIOINFORMATICS · OCTOBER 2001

Impact Factor: 2.63 · DOI: 10.1002/prot.1126 · Source: PubMed

3 AUTHORS, INCLUDING:

Sergei Y Venyaminov
Mayo Foundation for Medical Education an…
130 PUBLICATIONS **3,336** CITATIONS
SEE PROFILE

John Francis Hedstrom
Luther College
13 PUBLICATIONS **203** CITATIONS
SEE PROFILE

PROTEINS: Structure, Function, and Genetics 45:81–89 (2001)

Analysis of the Segmental Stability of Helical Peptides by Isotope-Edited Infrared Spectroscopy

S. Yu. Venyaminov,[1]* J.F. Hedstrom,[2] and F.G. Prendergast[1]
[1]*Department of Biochemistry and Molecular Biology, Mayo Foundation Rochester, Minnesota*
[2]*Chemistry Department, Luther College, Decorah, Iowa*

ABSTRACT **Isotope-edited infrared spectroscopy has the ability to probe the segmental properties of long biopolymers. In this work, we have compared the infrared spectra of a model helical peptide (^{12}C) Ac-W-(E-A-A-A-R)$_6$-A-NH$_2$, described originally by Merutka et al. (Biochemistry 1991;30: 4245–4248) and three derivatives that are ^{13}C labeled at the backbone carbonyl of alanines. The locations of six isotopically labeled alanines are at the N-terminal, C-terminal, and the middle two repeating units of the peptide. Variation in temperature from 1° to 91°C transformed the peptides from predominantly helical to predominantly disordered state. Amplitude and position of the infrared amide I′ absorption bands from ^{12}C- and ^{13}C-labeled segments provided information about the helical content. Temperature dependence of infrared spectra was used to estimate segmental stability. As a control measure of overall peptide stability and helicity (independent of labeling), the temperature dependence of circular dichroism spectra in the far-UV range at identical conditions (temperature and solvent) as infrared spectra was measured. The results indicate that the central quarter of the 32 amino acids helix has the maximal helicity and stability. The midpoint of the melting curve of the central quarter of the helix is 5.4 ± 0.8°C higher than that of the termini. The N-terminal third of the helix is more helical and is 2.0 ± 1.4°C more stable than the C-terminus. Proteins 2001;45:81–89.**

Key words: helical peptide; isotope labeling; circular dichroism; infrared spectra; temperature dependence; segmental stability

INTRODUCTION

Helices are the most common and stable elements of the regular secondary structure in globular and fibrillar proteins; they are internally hydrogen bonded and exist as autonomous folding units.[1] On average, about one-third of the residues in a broad set of globular proteins are in a helical conformation.[2]

Model α-helix-forming peptides have been extensively studied[3–8] in an attempt to understand the principles governing secondary structure formation and stability of peptides and proteins. Marqusee and Baldwin[3] were the first to investigate the helix-forming properties of short Ala-based peptides. Using circular dichroism (CD) spectroscopy, they monitored the helix-stabilizing effect of variably spaced E/K salt bridges; later, they employed nuclear magnetic resonance (NMR) spectroscopy to quantify the positional dependence and the strength of Q/D side-chain interaction on the stabilization of helical peptides.[4] Park et al.[5] used CD to examine the structural effects of various X-residue substitutions in the helical peptide, Ac-Y-(E-A-A-A-K)-(E-A-X-A-K)-(E-A-A-A-K)-A-NH$_2$ and to study the effects of pH and ionic strength on helix stability. In an earlier study,[6] they had shown that an E/R rather than E/K ion-pair—and various others—provided the most favorable charge-charge interaction for stabilizing the helical state.[7] The helix-forming peptide, Ac-W-(E-A-A-A-R)$_3$-A-NH$_2$, was also investigated[8] using ^{13}C NMR and CD to study the effects of pH, ionic strength, and temperature on its helicity. It was shown that the thermal dependence of the NMR parameters correlates with CD measurements of a two-state helix-coil transition, with the helical structure stabilized by backbone hydrogen bonds, the E/R salt bridges, and the capped helical ends.

Fourier transform infrared (FT-IR) spectroscopy has also proved to be a valuable tool for secondary structure determination of peptides and proteins and has been used to monitor steady-state structure[9] or kinetics of folding-unfolding transitions.[10,11] We employed IR spectroscopy[12] to study the length and temperature-dependence of spectral characteristics for Stellwagen's helix-forming peptides,[6] Ac-W-(E-A-A-A-R)$_n$-A-NH$_2$, with different length (n = 1–7). Our results demonstrated the usefulness of 2D analysis in the deconvolution and interpretation of spectral changes consequent upon the helix-coil transition. However, both IR and CD spectroscopy are low-resolution techniques that yield only overall structural information. Structural data on the level of individual residues are available from NMR, but this method has limitations in time resolution (the microsecond range) and assignment of the signal to individual Ala residue in alanine-based helix-forming peptides is very difficult unless specific residues are isotope enriched.

Grant sponsor: USPHS; Grant number: GM34847.

*Correspondence to: Sergei Yu. Venyaminov, Department of Biochemistry and Molecular Biology, Mayo Foundation 200 First Street SW, Rochester, MN 55905. E-mail: venyaminov.sergei@mayo.edu

Received 16 February 2001; Accepted 12 June 2001

TABLE I. Peptides Used for Spectral Measurements[†]

Sequence	State of ^{13}C labeling
Ac-W-(E-A-A-A-R)$_6$-A-NH$_2$	Unlabeled (^{12}C)
Ac-W-(E-<u>A-A-A</u>-R)$_2$-(E-A-A-A-R)$_4$-A-NH$_2$	^{13}C labeled N-terminal segment
Ac-W-(E-A-A-A-R)$_2$-(E-<u>A-A-A</u>-R)$_2$-(E-A-A-A-R)$_2$-A-NH$_2$	^{13}C labeled middle segment
Ac-W-(E-A-A-A-R)$_4$-(E-<u>A-A-A</u>-R)$_2$-A-NH$_2$	^{13}C labeled C-terminal segment

[†]Underlined alanines are ^{13}C labeled at the backbone carbonyl. All peptides have acetylated (Ac) N-terminal Trp and amidated (NH_2) C-terminal Ala.

Isotope-edited IR spectroscopy provides new possibilities for resolution enhancement on the level of individual peptides[13] or even individual residues.[14,15] Complete labeling of one peptide or protein at the backbone carbonyl of constituent amino acid residues allows independent examination of labeled and unlabeled parts of a peptide.

We have now used isotope-edited IR spectroscopy to probe the segmental properties of an alanine-based α helical peptide. We labeled different segments of the peptide and measured their helicity and temperature stability over a large temperature range, 1–91°C, and were able thereby to examine the labeled and unlabeled segments independently. The selected peptide, Ac-W-(E-A-A-A-R)$_6$-A-NH$_2$, has a high helicity and midpoint of temperature transition from predominantly helical to predominantly unordered structure-at ~48°C. CD spectroscopy was used as a control to monitor helicity and overall helix stability. These measurements allowed direct quantitative comparisons of the difference in stability and helicity between the central segment of a helical peptide and the N- and C-termini.

MATERIALS AND METHODS

Peptides were synthesized by use of an FMOC (9-fluorenyl-methoxycarbonyl)-based strategy and purified by reverse phase HPLC. Peptide purity and molecular weight, assessed by time of flight mass spectrometry and were found to be within 1 m/z of the expected values. The following peptides were used for spectral measurements (Table I).

The peptides were lyophilized several times out of 0.1 M HCl to remove residual TFA, which absorbs in the infrared range of interest at ~1,673 cm^{-1}. After this, dried samples were dissolved in water and the pH was adjusted to 7.0 with NaOH. The peptides were lyophilized to remove water (H_2O) and subsequently lyophilized twice out of D_2O to effect complete proton to deuterium exchange. For spectral measurements, the peptide samples were dissolved in 10 mM deuterated phosphate buffer and adjusted to 50 mM NaCl. CD and FT-IR spectral measurements were conducted in 10 mM NaPhosphate, 50 mM NaCl, pH 7.0 (D_2O), at a peptide concentration of 0.5–1 mg/mL and ~20 mg/mL, respectively.

The concentrations were determined using a DU-640 spectrometer (Beckman, Fullerton, CA) with an absorption bandwidth of 1.5 nm. Rectangular quartz cell with a path length of 1.02 mm was used for concentration measurement of CD samples and a demountable short path rectangular cell of 92 μm for IR samples. Molar absorptivity for Trp at 280 nm was assumed to be 5,579 $M^{-1} \cdot cm^{-1}$ (25°C). Before calculating the concentration, all spectra were corrected for turbidity by plotting the dependence of the log of the absorbance of the solution vs. the log of the wavelength and extrapolating the linear dependence between these quantities in the range 340–440 nm to the absorption range 240–300 nm. The extrapolated value at the wavelength of maximum absorbance was then subtracted from the measured value. The scatter correction routine of DU-640 was used for this purpose.

CD spectra were collected on a J-710 spectropolarimeter (JASCO, Japan) continuously purged by N_2 and equipped with a temperature control system CTC-345. Far-UV (185–240 nm) temperature-dependent measurements were performed at a bandwidth of 2 nm using a U-type quartz cell of path length 0.148 mm (volume 45 μL) and a home-made cell holder. CD spectra were recorded using 5 accumulations, each at scan speed of 20 nm/min and a response time of 2 s. CD spectra were collected at 16 different temperatures with a 6° interval from 1 to 91°C. The continuous temperature dependence of the ellipticity at 222 nm was measured using a scan rate of 50°C/h and a response time of 8 s. Solvent evaporation was prevented by placing a drop of oil that had been repeatedly boiled in water to remove water soluble impurities on top of the sample in the cell. The position of the temperature sensor of the CTC-345 unit was adjusted in the water hose about 1 m *after* the cell holder, so that the temperature gradient between the cell holder and the solution in the cell at a scan rate of 50°C/h was partially compensated for by the temperature gradient between the sensor and the cell holder. Additionally, the temperature inside the cell was calibrated by inserting the thermocouple in a similar U-type cell with a path length of ~0.5 mm. The changes of CD spectra were totally reversible after sample heating. CD spectra were smoothed by JASCO noise reduction routine. Spectral data are presented as molar ellipticity per residue.

IR spectra at resolution 2 cm^{-1} were measured with FTS-40 FTIR spectrometer (Digilab) continuously purged by N_2 and equipped with a DTGS detector. A home-made shuttle system and a thermostated brass block, which holds both sample (path length of 42.2 μm, volume 24 μL) and matched reference (41.4 μm) CaF_2 cells, were used for IR spectra measurements. The shuttle system, the construction of IR cells, as well as optical subtraction of solvent absorbance, have been described previously.[16] The shuttle system was programmed for 20 mechanical steps between sample and reference with 10 spectra accumu-

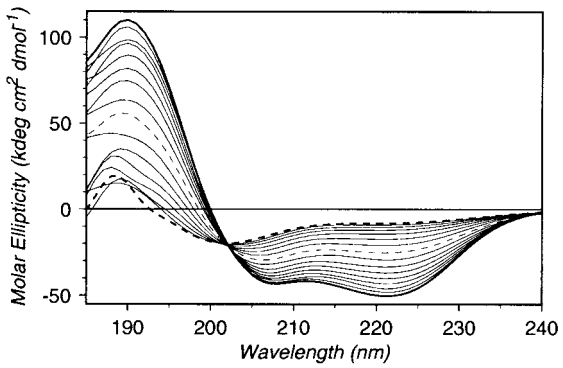

Fig. 1. CD spectra of C-terminal ^{13}C labeled peptide at 16 different temperatures between 1 and 91°C (6° interval). Thick line, 1°C; thin dotted line, 49°C; thick dotted line, 91°C. Buffer, 10 mM NaPhosphate, 50 mM NaCl, pH 7.0 (D_2O); peptide concentration (per residue), 4.85 mM; cell path length, 0.148 mm.

lated per step (200 spectra for each sample and reference within 17 min). Temperature was varied by use of an RTE-111 Neslab circulating bath; a thermal probe connected to the IR cell holder was used to measure the temperature. The procedure involved the collection of spectra for each peptide at 16 different temperatures through the temperature range of 1 to 91°C. To prevent solvent evaporation and contact of the atmospheric water vapor with solvent, the cell's sealing surface was lubricated with mineral oil dissolved in chloroform prior to cell assembly. As a result, the changes of the sample's IR spectra were 100% reversible even after prolonged exposure to high temperature. No correction was made for the contribution of sharp bands originating from atmospheric water vapor absorbance; these bands were practically eliminated by using the shuttle system for collecting spectra. Also no noise reduction needed to be applied to the measured IR spectra. The only IR spectra modification that was done, was the subtraction from all spectra the absorption value at 1,800 cm^{-1}. This nullification of all spectra at 1,800 cm^{-1} compensates for small, temperature-dependent shifts in spectra background that probably originated from the temperature dependence of the refractive index of CaF_2 and/or the solution. The absence of a concentration dependence of spectral properties for IR samples (concentration ~20 mg/mL) relative to the spectral properties for CD samples (concentration ~1 mg/mL) was confirmed by CD spectra measurements in the far-UV spectral range in 7.0 μm CaF_2 IR cell. The IR data are presented in units of molar absorptivity per residue.

RESULTS AND DISCUSSION

CD spectra in the far-UV range for the unlabeled sample and three ^{13}C labeled derivatives (Table I) were measured as a control of the overall helicity and stability independent of ^{13}C labeling of studied peptides. Figure 1 presents, as an example, the results of such measurements for C-terminal ^{13}C labeled peptide at 16 different temperatures between 1° and 91°C. It is possible to see that CD spectra on Figure 1 at low temperatures are typical for samples with very high helical content. At 1°C, it displays a maximum at 189.7 nm with a mean residue ellipticity [θ] of 109.0 kdeg · cm^2 · $dmol^{-1}$, minima at 221.4 nm with $-[\theta]$ = 50.0 kdeg · cm^2 · $dmol^{-1}$ and $-[\theta]_{207.6}$ = 41.0 kdeg · cm^2 · $dmol^{-1}$. An increase in temperature leads to a structural transition from high to low helicity, which is accompanied by significant changes in the shape of CD spectra and shows an isobestic point close to 203 nm characteristic[17] for the helix-unordered structure transition.

The thermal stability of the four peptides was determined by measuring the continuous temperature dependence of the ellipticity at 222 nm over the range 0° to 92°C (data not shown). The peak maximum for the first derivative or the crossover point for the second derivative of this sigmoidal curve determines the midpoint of sample melting.

Table II provides the results obtained from an analysis of the CD data. The errors in Table II and also in Tables III and IV are the standard deviations obtained from two measurements of each sample (additionally, each peptide sample was independently synthesized at least twice). The very small errors indicate the high repeatability of the quantitative spectral measurements. Table II shows seven spectral parameters and melting temperature for four peptides. Five values (the positions of positive [~190 nm] and negative [~221 nm] peaks in CD spectra, the crossover point, the ratio of molar ellipticity for positive peak over negative peak, as well as stability), which do not depend on amplitude of ellipticity, coincide very well for all samples. The absolute value of the ellipticity at ~190 and ~221 nm at 1°C, for states with high helicity, and at 91°C (~221 nm), for predominantly unordered states, are very close for the first three peptides but only 83% of those for the C-terminus labeled peptide. The interpretation of this result as higher helicity for the latter sample has to be rejected on the basis of the absence of any difference in the shape of the CD spectra in the far-UV range for all peptides, that is, the same max to min ellipticity ratio, positions of maximum, crossover point, and minimum are noted. Because in all cases the same CD cell was used, the only other possible reason for this difference could be uncertainty in concentration determination. We use the same molar absorptivity for Trp in all cases, and for some reason it seems that for the C-terminus labeled peptide Trp absorptivity is lower. We have no explanation for this apparent effect.

Thus, from the CD data one can see the similarity of optical properties of all four helical peptides studied. This is expected for electronic transitions, which have to be insensitive to isotope labeling of molecules (cf. vibrational transitions). A correction of the concentration for C-terminus labeled peptide was applied to adjust the amplitude of the IR spectra (see below). This led to more consistent interpretations of the IR data.

IR spectra in the range of the amide I′ absorbance band (a stretching of the C═O bond) for ^{13}C-labeled, at the backbone carbonyl, peptides could be used independently of unlabeled parts for monitoring the different physical properties of the labeled and unlabeled segments. The

TABLE II. Spectral Parameters and Stability Derived From CD Data†

Parameter	T, (°C)	Unlabeled peptide	N-terminus labeled	Middle labeled	C-terminus labeled
λ_{max} (nm)	1	189.8 ± 0.2	189.5 ± 0.4	189.6 ± 0.6	189.7 ± 0.4
			Avg. = 189.7 ± 0.1		
$[\theta]_{max}$ (kdeg · cm^2 · dmol^{-1})	1	90.3 ± 0.7	91.1 ± 0.7	88.8 ± 0.6	109.0 ± 1.2
			Avg. = 90.1 ± 1.0; 90.1/109.0 = 0.83		
$\lambda_{[\theta]=0}$ (nm)	1	200.0 ± 0.1	200.0 ± 0.1	200.0	199.9 ± 0.1
			Avg. = 200.0 ± 0.05		
λ_{min} (nm)	1	221.3 ± 0.2	221.2 ± 0.2	220.9 ± 0.1	221.4 ± 0.4
			Avg. = 221.2 ± 0.2		
$-[\theta]_{min}$ (kdeg · cm^2 · dmol^{-1})	1	41.6 ± 0.3	41.9 ± 0.2	40.7 ± 0.4	50.0 ± 0.3
			Avg. = 41.4 ± 0.5; 41.4/50.0 = 0.83		
$-[\theta]_{max}/[\theta]_{min}$	1	2.17 ± 0.02	2.18 ± 0.01	2.18 ± 0.03	2.18 ± 0.01
			Avg. = 2.18 ± 0.005		
$-[\theta]_{min}$ (kdeg · cm^2 · dmol^{-1})	91	6.7 ± 0.1	6.5 ± 0.1	6.3 ± 0.1	7.8 ± 0.3
			Avg. = 6.5 ± 0.2; 6.5/7.8 = 0.83		
T_m (°C)	—	48.7 ± 1.4	49.7 ± 0.2	48.7 ± 1.0	47.0 ± 1.9
			Avg. = 48.5 ± 1.0		

†λ_{max}, wavelength of maximum at ~190 nm; $[\theta]_{max}$, molar ellipticity at λ_{max}; $\lambda_{[\theta]=0}$, crossover point; λ_{min}, wavelength of minimum in the spectral range of 220–222 nm; $[\theta]_{min}$, molar ellipticity at λ_{min}; T_m (°C), midpoint of temperature dependence of molar ellipticity at 222 nm.

TABLE III. Spectral Parameters and Stability Derived From Amide I′ (^{12}C)†

Parameter	T, (°C)	Unlabeled peptide	N-terminus labeled	Middle labeled	C-terminus labeled
ν_{max} (cm^{-1})	1	1,630.9 ± 0.1	1633.9	1,635.8	1,632.9
		****	*,*	*	*,**
ε_{max} (M^{-1} · cm^{-1})	1	640 ± 65	443 ± 2	438 ± 2	(540 ± 13) × 0.83 = 448 ± 11
		****	*,*	*	*,**
			Avg. = (443 ± 5) × 32/26 = 545 ± 6		
ν_{max} (cm^{-1})	91	1,646.6 ± 0.5	1,647.6 ± 0.3	1,648.1 ± 0.2	1,647.3 ± 0.2
			Avg. = 1,647.4 ± 0.5		
ε_{max} (M^{-1} · cm^{-1})	91	392 ± 43	302 ± 4	303 ± 2	(365 ± 8) × 0.83 = 303 ± 7
			Avg. = (303 ± 1) × 32/26 = 373 ± 1		
$\varepsilon_{1°C}/\varepsilon_{91°C}$	1/91	1.63 ± 0.02	1.467	1.445 ± 0.005	1.479 ± 0.005
		****	*,*	*	*,**
T_m (°C)	—	45.4 ± 0.3	46.1 ± 0.6	41.5 ± 0.4	46.2 ± 0.5
				*	

†λ_{max}, wavenumber of maximum of the amide I′ absorbance band belonging to unlabeled peptide groups (^{12}C); ε_{max}, molar absorptivity at λ_{max}; $\varepsilon_{1C}/\varepsilon_{91C}$, ratio of molar absorptivity of the amide I′ at 1°C and 91°C; T_m (°C), midpoint of temperature dependence of molar absorptivity at 1658 cm^{-1}; *, helicity and stability measure (**** maximal value; * minimal value; *** and ** intermediate values).

^{13}C-isotope mass effect resulted in a shift of the amide I′ band by ~40 cm^{-1} to lower wavenumbers relative to the position of the band for the unlabeled part of the peptide. At the same time, the width at half height of the amide I/I′ bands for helical peptides[18,19] is equal to 32–37 cm^{-1}, for β sheet samples is several times smaller,[18,20] and for unordered structure[18,20] is equal to 42–55 cm^{-1}. This led to very good resolution of the amide I′ bands for the ^{13}C labeled and unlabeled parts of segments that had regular ordered secondary structure.

The three curves in Figure 2 illustrate absorbances for solution, solvent (both corrected on the reflection from CaF_2 window), and sample (corrected for absorbance of solvent) in the spectral range of 1,000–4,000 cm^{-1}. The absorbance band at 3,840 cm^{-1} is due to the combination of stretching and bending vibrations, at 2,504 cm^{-1}, to stretching, at 1,555 cm^{-1}, to a combination of bending vibration and librations, and at 1,209 cm^{-1} to bending vibrations of D_2O molecules.[16] The band at 3,404 cm^{-1} is due to the stretching of O—H and a shoulder at 1,462 cm^{-1} to a combination of bending and libration vibration of H—O—D molecules[16] (from traces of H_2O in D_2O). The absorption curves of the sample, corrected for solvent absorbance, have two amide bands: the amide I′, maxima at 1,633 cm^{-1} (^{12}C) and at 1,598 cm^{-1} (^{13}C), and the amide II′, two components in the range of 1,440–1,475 cm^{-1}. Absorbance bands, belonging to peptide C—H vibrations, occur at 2,800–3,000 cm^{-1} (stretching) and 1,380–1,410 cm^{-1} (bending). Figure 2 shows practically ideal compensation for solvent absorption and proves the correctness of IR spectra measurement for the sample, particularly in the spectral range of the amide I′ and II′ bands. The absence of the amide A (N—H stretching mode) band at ~3,300 cm^{-1} demonstrates a complete (better than 99%) H—D exchange of peptide groups.

Figure 3 exhibits IR spectra of unlabeled [Fig. 3(A)] and C-terminus ^{13}C labeled [Fig. 3(B)] peptides in the two spectral ranges: 1,270–1,500 (Fig. 3, left panel) and 1,530–1,730 cm^{-1} (Fig. 3, right panel). The upper curves display spectra in molar absorptivity units at 16 different tempera-

TABLE IV. Spectral Parameters and Stability Derived From Amide I′ (^{13}C)†

Parameter	T, (°C)	N-terminus labeled	Middle labeled	C-terminus labeled
ν_{max} (cm^{-1})	1	1,596.2 **	1,596.0 ± 0.1 ***	1,598.2 *
ε_{max} ($M^{-1} \cdot cm^{-1}$)	1	333 ± 11 **	350 ± 4 ***	(376 ± 3) × 0.83 = 312 ± 2 *
$\varepsilon_{13C}/\varepsilon_{12C}$	1	0.752 ± 0.002 **	0.799 ± 0.005 ***	0.696 ± 0.014 *
T_m (°C)	—	44.4 ± 0.6 **	46.9 ± 0.4 ***	42.4 ± 0.8 *

†ν_{max}, wavenumber of maximum of the amide I′ absorbance band belonging to the labeled peptide groups (^{13}C); ε_{max}, molar absorptivity at ν_{max}; $\varepsilon_{13C}/\varepsilon_{12C}$, ratio of molar absorptivity of amide I′ belonging to labeled (^{13}C) and unlabeled (^{12}C) peptide groups; T_m (°C), midpoint of temperature dependence of molar absorptivity at 1,596 cm^{-1}; *, helicity and stability measure (*** maximal value; * minimal value; ** intermediate value).

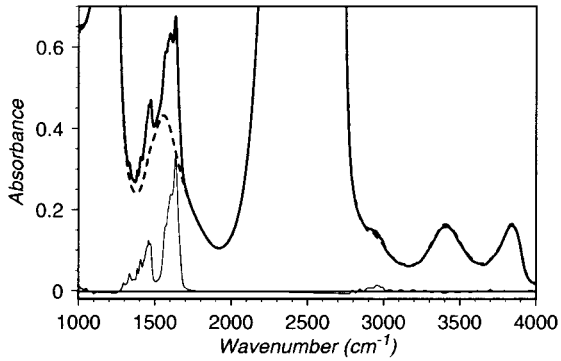

Fig. 2. IR spectra of C-terminal ^{13}C labeled peptide at 25°C. Thick line, solution vs. CaF_2 (10 mm); thick dotted line, solvent vs. CaF_2 (10 mm); thin line, solution vs. solvent. Buffer, 10 mM NaPhosphate, 50 mM NaCl, pH 7.0 (D_2O); peptide concentration (per residue), 0.1575 M; sample cell path length, 0.0422 mm, reference cell (with buffer) 0.0414 mm.

tures, the lower display differences between spectra at the current temperature and 91°C. It is seen from Figure 3(A) that at low temperatures (predominantly helical state), the amide I′ band of unlabeled peptide has maximal value for molar absorptivity and minimal for peak position. An increase in temperature leads to helix-unordered structure transition and is accompanied by a decrease in amplitude and a shift to the higher wavenumbers of the amide I′ band. Thus, the position and the amplitude of the amide I′ absorbance band can be used for comparative estimation of helicity in studied samples. One can see in Figure 3 the absence of a good isobestic point in the range 1,640–1,650 cm^{-1}. The possible reason for this is the temperature dependence of the position, amplitude, and width of the amide I′ mode for helical and unordered states of the peptide backbone. According to Graff et al.,[12] the temperature dependence of band position for both conformations has about the same slope and the amide I′ band shifts to higher wavenumbers with a temperature increase. In contrast, CD spectra in Figure 1 have a good isobestic point at 203 nm. A reasonable explanation of this result is that there are opposite slopes of the temperature dependence of CD spectra in the far-UV range for ordered and unordered structures without significant shifts of wavelength.[21] The difference spectra in the range of the amide I′ band show a positive peak at 1,628 cm^{-1} (helicity decrease at high temperatures) and a negative one at 1,658 cm^{-1} (increase of unordered structure content). First or second derivatives of the changes at 1,628 and 1,658 cm^{-1} with temperature are essentially the same (data not shown); both peaks have midpoints of temperature dependence at 45.4 ± 0.3°C. The last value is smaller than that derived from CD data at 48.5 ± 1.0°C. The CD value is closer to the "real" value because the calibration of temperature in this case was done by insertion of a thermocouple inside the CD cell; in the IR case the thermocouple measured the temperature of the cell holder.

In addition to the amide I′ absorption band in the range 1,530–1,730 cm^{-1} in Figure 3(A), are the bands belonging to absorbance of the side chain[22] of Glu, at 1,567 cm^{-1} and Arg, at 1,586 and 1,608 cm^{-1} (the last band is visible only at high temperature).‡ The position of these bands is indicated at 25°C, and it has its own temperature dependence,[12] irrespective of structure. For H_2O solutions,[24] these bands move to 1,560 cm^{-1} for Glu, and to 1,673 and 1,633 cm^{-1} for Arg. In the latter case, in contrast to D_2O solution, there is a very strong overlapping of Arg absorbance with the amide I band.

In the spectral range 1,270–1,500 cm^{-1} in Figure 3(A), one can see an additional absorbance of unlabeled peptides. It includes the amide II′ band with two components at 1,457 and 1,473 cm^{-1} (helical state at low temperatures) and two small shoulders at 1,427 and 1,448 cm^{-1}. At higher temperatures, in the course of the helix to unordered structure transition, two components of the amide II′ band with maxima at 1,444 and 1,464 cm^{-1} shift to

‡Hamm et al.[23] have examined by two-dimensional IR spectroscopy (in D_2O) a cyclic penta-peptide, which included Arg. The authors assigned the bands at 1,673, 1,648, 1,620, 1,610, and 1,584 cm^{-1} to the amide I′ modes of the five constituent peptide groups of the sample. They observed the strongest cross-peaks for the 1,610/1,584 cm^{-1} pair. However, as noted here the band at 1,584 cm^{-1} cannot reasonably be assigned to the amide I′ mode and, along with the band at 1,610 cm^{-1}, most likely belongs to the very strong absorbance of the Arg side chain. The integrated intensity of these two bands of the Arg side chain is more than 50% higher than those of the two components at 1,672 and 1,648 cm^{-1} of amide I′ band for an unordered structure.[20,22] Graff et al.[12] have also shown by 2D IR spectroscopy that there is high correlation between the 1,586 and 1,608 cm^{-1} modes of the Arg side chain in Arg-containing peptides.

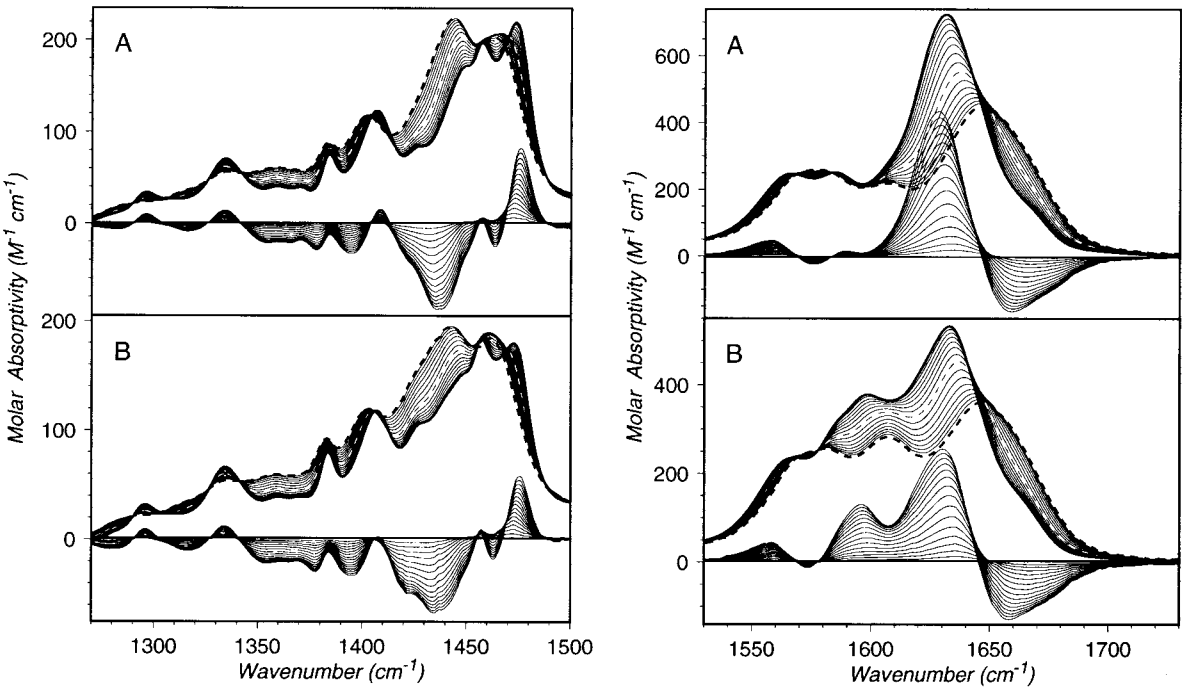

Fig. 3. IR spectra of unlabeled (**A**) and C-terminal ^{13}C labeled peptide (**B**) at 16 different temperatures between 1 and 91°C (6° interval) and 15 difference spectra (spectrum at current temperature minus spectrum at 91°C). Thick line, 1°C; thin dotted line, 49°C; thick dotted line, 91°C. Buffer, 10 mM NaPhosphate, 50 mM NaCl, pH 7.0 (D_2O); cell path length, 0.0422 mm; concentration (per residue), 0.1935 M for unlabeled and 0.1575 M for ^{13}C labeled peptide.

lower wavenumbers and become broader, but without big changes in their amplitudes. To the best of our knowledge, this is the first quantitative data for the amide II′ mode that have been compensated properly for solvent absorbance.

The band at 1407 cm^{-1}, —COO^- symmetric stretching mode,[23] shifts to 1402 cm^{-1} with decrease in intensity upon temperature increase. In difference spectra, these changes produce sigmoidal curves with a positive peak at 1,409, crossover point at 1,404, and a negative peak at 1,306 cm^{-1}. The C—H bending mode at 1,384 cm^{-1} decreases intensity without a change in band position at higher temperatures.

There are two unidentified absorption components at 1,296 and 1,334 cm^{-1} (at low temperatures) on the Figure 3(A). These bands cannot belong to the unexchanged amide III mode because of complete reversibility of their positions and amplitudes after prolonged heating. It may be possible that the 1,334 cm^{-1} band arises from a Trp side-chain mode.[25] The temperature increase leads to a decrease of the band absorbance and increase in absorbance between bands, without changes in position of band maximum. It is possible to see on the difference spectra two positive bands at 1,296 and 1,334 cm^{-1} and two negative bands at 1,284 and 1,316 cm^{-1}, with three crossover points at 1,290, 1,326, and 1,341 cm^{-1}.

Thus, the helix to unordered structure transition of the unlabeled polypeptide induced by increase in temperature is accompanied by significant changes in the shape and/or amplitudes of all amide bands. The molar absorptivity of the amide II′ is a factor of three smaller than that of the amide I′ in the helical state and two times smaller in the unordered state. Thus, the best signal to noise ratio (see also Fig. 2) for proteins and polypeptides in D_2O solution is obtained for the amide I′ absorbance band.

The example of IR spectra for the C-terminus ^{13}C-labeled peptide is given on the Figure 3(B). The only new feature, in comparison with the unlabeled sample, is the presence of the additional amide I′ band at 1,598 cm^{-1} and the slight difference in the shape of the amide II′ band (12% contribution of ^{13}C—O bending to the energy distribution of this mode[26]). The amide I′ absorption band component at 1,596–1,598 cm^{-1} was used to monitor the helicity and stability of the labeled segments and the main band at 1,630–1,636 cm^{-1} is employed to monitor these for the unlabeled parts of the four samples (see Table 1). Spectral parameters and stabilities derived from the amide I′ (^{12}C) and (^{13}C) bands are summarized correspondingly in Tables III and IV. All molar adsorptivity values for the C-terminus labeled peptides in both Tables were corrected by a factor of 0.83 (see Table II and discussion of CD data).

The parameters in Table III include the positions (ν_{max}) and amplitudes (ε_{max}) of the amide I′ for labeled and unlabeled samples, derived from the ^{12}C band at 1°C, that is, for the peptide in a predominantly helical state, and at 91°C for the predominantly unordered state. The lower ν_{max} and higher ε_{max} values indicate higher apparent helicity (according to IR data) for the unlabeled parts of the corresponding sample.

In the first row of Table III, the unlabeled peptide, with the longest ^{12}C α-helix, also has the highest apparent helicity. The C-terminus labeled peptide, with the ^{12}C

segment Ac-W-(E-A-A-A-R)$_4$-, on the N-terminus has the second highest apparent helicity, maximal for labeled samples. This can be interpreted as an indication that the ^{13}C-labeled C-terminus segment -(E-A-A-A-R)$_2$-A-NH$_2$ has the lowest helicity. The middle-labeled peptide has the lowest apparent helicity because, in this case, six central labeled alanines, which have the highest apparent helicity (see Table IV), interrupt the transition dipole coupling between ^{12}C peptide groups in C- and N-termini, and, as result, the peptide has two vibrationally independent short ^{12}C segments, -(E-A-A-A-R)$_2$-. The N-terminus labeled peptide has a higher helicity than the middle-labeled one. This is consistent with the data for other peptides.

The second row in Table III shows a molar absorptivity of the amide I′ band for the peptides. Because one has to use the peptide concentration for calculation of this value, an additional experimentally determined parameter, the interpretation of these data is not as straightforward as for the band position. After correction of the absorption value for the C-terminus labeled peptide with the factor 0.83 (see Table I), the molar absorptivity of the three labeled peptides practically coincides within the error of measurement. Conditionally, we distribute three labeled peptides according to the average values of their molar absorptivities. All values of molar absorptivity in this work were calculated per mole of peptide residue. Therefore, for comparison with unlabeled peptide, ^{12}C molar properties of labeled peptides have to be multiplied by 32/26 (six ALAs from 32 residues are ^{13}C labeled). The average value of the corrected molar absorptivity for labeled peptides is equal to $545 \pm 6\ M^{-1} \cdot cm^{-1}$, which is smaller than that for the unlabeled peptide, $640 \pm 65\ M^{-1} \cdot cm^{-1}$. Thus, the unlabeled peptide has the highest apparent helicity. Also, the big difference in molar absorptivity is evidence for the chain length dependence of the α-helix absorbance.[12,27,28]

Opposite to the helical state of these peptides, their optical properties in the state close to unordered, that is, at 91°C, are not chain-length dependent, and, as evident from Table III rows 3 and 4, the values of theirs ν_{max} and ε_{max} are very close. This fact can serve as a control for the consistency in experimental data at different conditions and is an independent demonstration of the validity of the concentration correction of molar absorptivity values for the C-terminus labeled peptide.

The next parameter in Table III (row 5) is the ratio of the amide I′ (^{12}C) absorbance at 1°C over absorbance at 91°C. It is a concentration-independent parameter, measured with high precision, and its value is proportional to the helical content of the studied samples (the value of the molar absorptivity at low temperatures is proportional to the helical content but at high temperatures, or in unordered state, has to be constant for any peptide). The values of this parameter correlate very well with position and amplitude of the amide I′ band (rows 1 and 2 in Table III).

The last parameter in Table III is the midpoint of the temperature dependence of molar absorptivity at 1,658 cm^{-1}. This parameter shows the melting temperature of unlabeled part (^{12}C) of peptides. We select this wavenumber to monitor melting of the unlabeled helical segments because at 1,628 cm^{-1} [compare Fig. 3(A) and (B)] in ^{13}C labeled samples, the absorbance of unordered ^{13}C segment, which increases with the temperature increase, contributes to absorbance at 1,628 cm^{-1} and interferes with absorbance of ^{12}C helix, which decreases with temperature increase. In the case of the unlabeled peptide, the monitoring of the temperature dependence at 1,628 and 1,658 cm^{-1} gives essentially the same result. It is seen from Table III, row 6, that only the middle-labeled peptide gives the average midpoint of temperature transition of the two terminus -(E-A-A-A-R)$_2$- short ^{12}C segments at 41.5 ± 0.4°C, which is different from the other samples. We were unable to distinguish melting behavior of the C-terminus + middle unlabeled segments, N-terminus + middle unlabeled segments, or totally unlabeled peptide, as all of these samples have the same average midpoint of melting at 45.9 ± 0.4°C. This result demonstrates the difference in stability of short [two pentamers, -(E-A-A-A-R)$_2$] and longer (four or six pentamers) helical segments.

Table IV gives spectral parameters and stability derived from amide I′ (^{13}C) for three labeled peptides. These parameters relate only to the short, -(E-A-A-A-R)$_2$-, α-helices. They include position, ν_{max}, and amplitude, ε_{max}, of the amide I′ band (^{13}C). As in the case of the amide I′ for ^{12}C peptide groups, the lower ν_{max} and the higher ε_{max} values indicate the higher helicity of this sample. The value of the ratio for absorbance at 1,596–1,598 cm^{-1} (the amide I′ for ^{13}C peptide groups) over absorbance at 1,631–1,636 cm^{-1} (the amide I′ for ^{12}C peptide groups), which is independent of concentration determinations, is proportional to the helicity of ^{13}C labeled segment. All three spectral parameters show the same pattern: the highest helicity for the middle-labeled, the second helicity for N-terminus labeled, and the lowest helicity for C-terminus labeled segment. The same results for stability give comparisons of midpoints for the temperature dependence of the amide I′ band (^{13}C) at ~1,597 cm^{-1}. These results are totally complementary with results derived from Table III.

One can see from Tables III and IV that the central segment of a 32-residue-long α-helix has the highest helicity and stability (Table IV, column for middle-labeled sample, all rows). The rest of the polypeptide has the lowest helicity and stability (Table III, column for middle-labeled sample, rows 1, 2, 5, and 6). Comparison of T_m values for the middle-labeled segment in Tables III (average stability of two-pentamer-long unlabeled segments on the N- and C-terminus) and IV (stability of two-pentamer-long labeled segment in the middle of the helix) shows that the difference in stability between the termini and the central segment is equal to 5.4 ± 0.8°C. It is incorrect to compare T_m values in Table III because in this case one compares helices with different lengths. The unlabeled peptide has a six-pentameter-long helix, middle-labeled peptide—two segments of a two-pentamer-long, and a C- and N-terminus—four-pentamer-long ^{12}C helices. Comparison of the two columns for the C- and N-terminus labeled segments in Table IV (all rows) shows that the N-terminus is more helical and more stable than C-terminus. Table III

shows just the opposite situation for the rest of peptide (^{12}C): the C-terminus labeled segment is more helical than the N-terminus labeled segment (Table III, first two rows). The difference in stability between two termini is equal to 2.0 ± 1.4°C (compare the two columns in Table IV).

One can see a very high degree of consistency among all of the data presented in this paper. The data in this paper also clearly demonstrate vibrational decoupling of the ^{13}C-labeled peptide group/s from the unlabeled groups. Resonance interactions of transition dipoles are responsible for a significant part of all bonded and nonbonded interactions and determine the geometrical sensitivity of the spectral properties of peptides and proteins, which allows the use of IR (and another types of optical spectroscopy) for structural determinations.[26,29] The ^{13}C labeling of very few (one or two) residues is insufficient for interpretation of vibrational features of the labeled residues in terms of secondary structure, even if they are physically within a segment of defined secondary structure. From our data, it appears that a minimum of three consecutive residues is required for an effective display of helical characteristics of a labeled segment.

CONCLUSION

This work has shown that for an α-helix consisting of 32 amino acid residues:

1. The central quarter of the helix has the maximal helicity and stability. The midpoint of the melting curve of the central quarter of the helix is 5.4 ± 0.8°C higher than that of the termini.
2. The N-terminal third of the helix is more helical and is 2.0 ± 1.4°C more stable than the C-terminus.

Accordingly, in an α-helix, the C-terminal segment melts faster than the N-terminal segment and hence in the course of the heat denaturation the effective center of the α-helix moves progressively toward the N-terminus.

Several questions may be raised: are these conclusions related only to the chosen polypeptide model, or are they relevant to other models or even to helical segments in globular proteins? If so, what differences in structure and/or stability of the two termini determines this asymmetry in any α helical segment?

The data presented in this work agree with data published previously for shorter polypeptide models[8] with similar or analogous sequences, but also for polypeptides with totally different amino acid sequences.[14,30,31] The data are also in accord with the results of molecular dynamics simulations of peptides corresponding to residues 132–149 of the H-helix of myoglobin[32] or of a ribonuclease S-peptide analogue.[33,34] These molecular dynamics simulations have indicated a higher stability of the N-terminus as compared with the C-terminus, unfolding occurring from C toward the N-terminus, and the presence of transient intermediates containing $i \rightarrow i + 3$ hydrogen bonds. All of the above-mentioned data, which have been reviewed by Bolin and Millhauser,[35] and the data we have now presented can be used as definitive evidence that the asymmetry in structure and stability are intrinsic properties of an *isolated* helix.

On the other hand, an analysis of structures in globular proteins[35,36] also shows, according to X-ray data, that the several residues with conformation very close to one turn of a 3_{10}-helix can be found very often on the C-terminus of α-helices. Thus, the presence on the C-terminal "exit" from helical segment structure close to 3_{10}-helix is characteristic of an isolated helix, and also of a helix that is connected with other element of secondary structure in globular proteins. The 3_{10}-helix is stabilized by $i \rightarrow i + 3$ hydrogen bonds, which have more geometrical distortion than the $i \rightarrow i + 4$ pattern of an α-helix. Side-chain packing is also rather unfavorable because steric hindrance is present in this structure. As a result, the C-terminus in an α-helix is necessarily more distorted and less stable than the N-terminus. A single turn of a 3_{10}-helix at the C-terminus an α-helix can serve as interface between α-helix and consecutive loop because its diameter has a value that is intermediate between that of an α helical segment and that of an extended polypeptide chain.

We conclude that the principles of helix stability drawn from the present data are relevant to any polypeptide model for isolated helices in solution and probably also for helical segments in proteins.

ACKNOWLEDGMENTS

We thank Dr. A. V. Efimov for helpful discussion, Ms. A. Svatikova for participation in measurements of same CD spectra, and Dr. M.C. Moncrieffe and Ms. M.S. Veniaminova for assistance in the preparation of the manuscript.

REFERENCES

1. Parthasarathy R, Chaturvedi S, Go K. Design of α-helical peptides: their role in protein folding and molecular biology. Prog Biophys Mol Biol 1995;64:1–54.
2. Barlow D, Thornton JM. Helix geometry in proteins. J Mol Biol 1988;201:601–619.
3. Marqusee S, Baldwin RL. Helix stabilization by $Glu^- \cdots Lys^+$ salt bridges in short peptides of de novo design. Proc Natl Acad Sci USA 1987;84:8898–8902.
4. Huyghues-Despointes BMP, Klinger TM, Baldwin RL. Measuring the strength of side-chain hydrogen bonds in peptide helices: the Gln · Asp (i, $i + 4$) interaction. Biochemistry 1995;34:13267–13271.
5. Park S, Shalongo W, Stellwagen E. Modulation of the helical stability of a model peptides by ionic residues. Biochemistry 1993;32:12901–1905.
6. Merutka G, Shalongo W, Stellwagen E. A model peptide with enhanced helicity. Biochemistry 1991;30:4245–4248.
7. Shalongo W, Stellwagen E. Incorporation of pairwise interactions into the Lifson-Roig model for helix prediction. Protein Sci 1995;4:1161–1166.
8. Shalongo W, Dugad L, Stellwagen E. Analysis of the thermal transitions of a model helical peptide using ^{13}C NMR. J Am Chem Soc 1994;116:2500–2507.
9. Surewicz WK, Mantsch HH, Chapman D. Determination of protein secondary structure by Fourier transform infrared spectroscopy: a critical assessment. Biochemistry 1993;32:389–394.
10. Gilmanshin R, Williams S, Callender RH, Woodruff WH, Dyer RB. Fast events in protein folding: relaxation dynamics and structure of the I form of apomyoglobin. Biochemistry 1997;36:15006–15012.
11. Williams S, Causgrove T, Gilmanshin R, Fang KS, Callender RH, Woodruff WH, Dyer RB. Fast events in protein folding: helix melting and formation in small peptide. Biochemistry 1996;35:691–697.

12. Graff GK, Pastrana-Rios B, Venyaminov SY, Prendergast FG. The effects of chain length and thermal denaturation on helix-forming peptides: a mode-specific analysis using 2D FT-IR. J Am Chem Soc 1997;119:11282–11294.
13. Zhang M, Fabian H, Mantsch HH, Vogel HJ. Isotope-edited Fourier transform infrared spectroscopy studies of calmodulin's interaction with its target peptides. Biochemistry 1994;33:10883–10888.
14. Decatur SM, Antonic J. Isotope-edited infrared spectroscopy of helical peptides. J Am Chem Soc 1999;121:11914–11915.
15. Andersen NH, Dyer RB, Fesinmeyer RM, Gai F, Liu Z, Neidigh JW, Tong H. Effect of hexafluoroisopropanol on the thermodynamics of peptide secondary structure formation. J Am Chem Soc 1999;121:9879–9880.
16. Venyaminov SY, Prendergast FG. Water (H_2O and D_2O) molar absorptivity in the 1000–4000 cm^{-1} range and quantitative infrared spectroscopy of aqueous solutions. Anal Biochem 1997;248:234–245.
17. Greenfield N, Fasman GD. Computed circular dichroism spectra for the evaluation of protein conformation. Biochemistry 1969;8:4108–4116.
18. Venyaminov SY, Kalnin NN. Quantitative IR spectrophotometry of peptide compounds in water (H_2O) solutions. II. Amide absorption bands of polypeptides and fibrous proteins in α-, β-, and random coil conformation. Biopolymers 1990;30:1259–1271.
19. Chirgadze YN, Brazhnikov EV. Intensities and other spectral parameters of infrared amide bands of polypeptides in the α-helical form. Biopolymers 1974;13:1701–1712.
20. Chirgadze YN, Shestopalov BV, Venyaminov SY. Intensities and other spectral parameters of infrared amide bands of polypeptides in the β- and random forms. Biopolymers 1973;12:1337–1351.
21. Privalov PL, Tiktopulo EI, Venyaminov SY, Griko YV, Makhatadze GI, Khechinashvili NN. Heat capacity and conformation of proteins in the denatured state. J Mol Biol 1989;205:737–750.
22. Chirgadze YN, Fedorov OV, Trushina NP. Estimation of amino acid residue side-chain absorption in the infrared spectra of protein solution in heavy water. Biopolymers 1975;14:679–694.
23. Hamm P, Lim M, DeGrado WF, Hochstrasser RM. The two-dimensional IR nonlinear spectroscopy of a cyclic penta-peptide in relation to its three-dimensional structure. Proc Natl Acad Sci USA 1999;96:2036–2041.
24. Venyaminov SY, Kalnin NN. Quantitative IR spectrophotometry of peptide compounds in water (H_2O) solutions. I. Spectral parameters of amino acid residue absorption bands. Biopolymers 1990;30:1243–1257.
25. Barth A. The infrared absorption of amino acid side chains. Prog Biophys Mol Biol 2000;74:141–173.
26. Krimm S, Bandekar J. Vibrational spectroscopy and conformation of peptides, polypeptides, and proteins. In: Anfinsen CB, Edsall JT, Richards FM, editors. Advances in protein chemistry. London, UK: Acad Press; 1986. p 181–365.
27. Kalnin NN, Baikalov IA, Venyaminov SY. Quantitative IR spectrophotometry of peptide compounds in water (H_2O) solutions. III. Estimation of the protein secondary structure. Biopolymers 1990;30:1243–1257.
28. Sreerama N, Venyaminov SY, Woody RW. Estimation of the number of α-helical and β-strand segments in proteins using circular dichroism spectroscopy. Protein Sci 1999;8:370–380.
29. Nevskaya NA, Chirgadze YN. Infrared spectra and resonance interactions of amide-I and II vibrations of α-helix. Biopolymers 1976;15:637–648.
30. Miick SM, Casteel KM, Millhauser GL. Experimental molecular dynamics of an alanine-base helical peptide determined by spin label electron spin resonance. Biochemistry 1993;32:8014–8021.
31. Silva RAG, Kubelka J, Bour P, Decatur SM, Keiderling TA. Site-specific conformational determination in thermal unfolding studies of helical peptides using vibrational circular dichroism with isotopic substitution. Proc Natl Acad Sci USA 2000;97:8318–8323.
32. Soman KV, Karimi A, Case DA. Unfolding of an α-helix in water. Biopolymers 1991;31:1351–1361.
33. Tirado-Rives J, Jorgensen WL. Molecular dynamics simulations of the unfolding of an α-helical analogue of ribonuclease A S-peptide in water. Biochemistry 1991;30:3864–3871.
34. Soman KV, Karimi A, Case DA. Molecular dynamics analysis of a ribonuclease C-peptide analogue. Biopolymers 1993;33:1567–1580.
35. Bolin KA, Millhauser GL. α and 3_{10}: The split personality of polypeptide helices. Acc Chem Res 1999;32:1027–1033.
36. Efimov AV. Standard structures in proteins. Prog Biophys Mol Biol 1993;60:201–239.